

# ZnO Nanoparticles Induced Male Reproductive Toxicity Based on the Effects on the Endoplasmic Reticulum Stress Signaling Pathway

This article was published in the following Dove Press journal:  
*International Journal of Nanomedicine*

Yizhou Tang<sup>1</sup>  
Bolu Chen<sup>1</sup>  
Wuding Hong<sup>1</sup>  
Ling Chen<sup>1,2</sup>  
Liyang Yao<sup>1</sup>  
Yu Zhao<sup>1</sup>  
Zoraida P Aguilar<sup>3</sup>  
Hengyi Xu<sup>1</sup>

<sup>1</sup>State Key Laboratory of Food Science and Technology, Nanchang University, Nanchang 330047, People's Republic of China; <sup>2</sup>The Second Affiliated Hospital of Nanchang University, Nanchang 330000, People's Republic of China; <sup>3</sup>Zystein, LLC., Fayetteville, AR 72704, USA

**Purpose:** The aim of this study was to evaluate the adverse effects of ZnO NPs on male reproductive system and explore the possible mechanism.

**Methods:** In this study, the effect of oral administration of 50, 150 and 450 mg/kg zinc oxide nanoparticles (ZnO NPs) in adult male mice was studied over a 14-day period.

**Results:** The results showed that the number of sperms in the epididymis and the concentration of testosterone in serum were decreased with an increased dose of ZnO NPs. Testicular histopathological lesions like detachment, atrophy and vacuolization of germ cells were observed. The results showed that increased dosage of ZnO NPs correspondingly up-regulated the IRE1 $\alpha$ , XBP1s, BIP, and CHOP ( $P < 0.05$ ) which are genes related to ER stress. These observations indicated that ZnO NPs had adverse effects on the male reproductive system in a dose-dependent manner possibly through ER stress. The expression of caspase-3 was significantly increased in all the treated groups ( $P < 0.001$ ), which reflected the possible activation of apoptosis. Additionally, there was significant down-regulation of the gene *StAR* ( $P < 0.05$ ), a key player in testosterone synthesis. When an ER-stress inhibitor salubrinal was administered to the 450 mg/kg ZnO NPs treatment group, the damages to the seminiferous tube and vacuolization of Sertoli and Leydig cells were not observed. Furthermore, the testosterone levels in the serum were similar to the control group after the subsequent salubrinal treatment.

**Conclusion:** It may be inferred that the ZnO NP's reproductive toxicity in male mice occurred via apoptosis and ER-stress signaling pathway.

**Keywords:** zinc oxide nanoparticles, male reproductive toxicity, endoplasmic reticulum stress

## Introduction

In recent years, various nanomaterials have been used in various commercial products including medicine, agriculture, animal husbandry, food industry, cosmetics and environmental protection, which made large impacts in human lives.<sup>1</sup> One of the most common NPs used is zinc oxide nanoparticles (ZnO NPs), which possess unique physical, chemical and antibacterial properties that have been harnessed in many products such as sunscreens in cosmetics, as textile coatings, antibacterial agents in food packaging, potential fertilizers, and some biomedical applications.<sup>2-4</sup> Moreover, ZnO NPs in commercial products inevitably gets released to the environment.<sup>5</sup> These possibly led to increased exposure to ZnO NPs, making safety a growing concern.<sup>6</sup> Various studies on the hazards of ZnO NPs

Correspondence: Hengyi Xu  
State Key Laboratory of Food Science and Technology, Nanchang University, 235 Nanjing East Road, Nanchang 330047, People's Republic of China  
Tel +86-791-8830-4447 ext 9520  
Fax +86-791-8830-4400  
Email kidyxu@163.com

have been published. In vitro toxicity of ZnO NPs found that ZnO NPs accumulated in cells which led to cell death through oxidative stress and inflammatory response.<sup>7</sup> ZnO NPs were internalized by Leydig cells and Sertoli cells that resulted in cytotoxicity in a time- and dose-dependent manner through the induction of apoptosis.<sup>8,9</sup> While ROS generation triggered by ZnO NPs could cause germ cell DNA damage and break the tight junction of Sertoli cells which compromised the integrity of the blood-testis barrier.<sup>10</sup> In vivo studies have revealed the ZnO NPs toxicity on experimental animals. ZnO NPs could affect the normal structure and function of the liver in mice, leading to inflammation and hyperemia in the lung,<sup>11</sup> even inducing anemia, stomach lesions, kidney atrophy, and eye damage.<sup>12</sup>

Infertility has affected 8–12% of the couples in the childbearing age around the world.<sup>13</sup> About half of these cases had been accounted to the males.<sup>14</sup> The male reproductive organ has been known to be susceptible to environmental stress that could come as external toxicants, vehicular pollutants, and even nanoparticles. It had been reported that nanoparticles could pass through the blood–testis barrier due to its small size,<sup>15,16</sup> which was exhibited by Mozaffari et al who found ZnO NPs in the testis of adult NMRI mice after exposure to ZnO NPs for a week, and compared with the control group, the sperm population of the experimental group was significantly lower and the sperm deformity rate was significantly elevated; in addition, they also discovered that ZnO NPs caused testicular sperm cell apoptosis.<sup>17</sup> Abbasalipourkabir et al showed that intraperitoneally injected ZnO NPs led to lower sperm count, slower motility and increased abnormality in male rats.<sup>18</sup> The study by Talebi et al using 50 and 300 mg/kg ZnO NPs resulted in a significant change in the following spermatogenic parameters: sperm number, motility, percentage of abnormality, seminiferous tubule diameter, seminiferous epithelium height and maturation arrest, which implied that ZnO NPs had testicular toxicity as well as negative impact on spermatogenesis.<sup>19</sup>

Currently, studies on the mechanisms of toxicity of nanomaterials focused on excessive production of reactive oxygen species (ROS) that caused oxidative stress.<sup>20,21</sup> The endoplasmic reticulum (ER) has been shown to be sensitive to ROS, and hence, ROS generation could induce excess accumulation of unfolded/misfolded proteins in the ER lumen.<sup>22–24</sup> ER stress when activated could promote protein folding/degradation, but it could also trigger apoptosis.<sup>25</sup> Yang et al found that exposure to ZnO NPs

induced oxidative stress and ER stress in the liver that led to apoptosis that induced liver injury.<sup>26</sup> Similarly, Kuang et al demonstrated that 30 nm ZnO NPs activated ER stress and the apoptosis pathway in the liver.<sup>27</sup> Corollary to these findings, it has been reported that the ROS-regulated PERK/eIF2 $\alpha$ /CHOP pathway played a vital role in bisphenol A-induced male reproductive toxicity.<sup>28</sup> Hence, ER stress induced by ROS may be involved in the male reproductive toxicity that could be caused by nanoparticles, but there is still a lack of relevant research in this area.

In this study, the adverse effects of ZnO NPs on the male reproductive system were evaluated by analyzing the testicular morphology changes, sperm count and testosterone level. The animal oral exposure study was carried out for 14 days to explore the intrinsic toxicity mechanism of ZnO NPs by monitoring levels of ER stress-related genes.

## Materials and Methods

### Characterization of ZnO NPs

ZnO NPs powder (30 nm  $\pm$  nm) was obtained from Xiya Reagent, LLC (Chengdu, China). The sizes of ZnO NPs were evaluated by field emission scanning electron microscopy (SEM) with an energy spectrometer (JSM 6701F, JEOL Ltd.).

### Animals and Experimental Design

Forty healthy male Kunming mice (6 weeks old, weight 22  $\pm$  2 g) were purchased from the experimental animal center of Nanchang University (Nanchang, China). All experiments were conducted under the direction of the Animal Care Review Committee of Nanchang university (approval number: 0064257) following the guidelines for ethical review of experimental animal welfare of China (GB/T35892-2018). Before the experiments, the mice were fed for a week in the laboratory animal room where the indoor temperature was maintained at 20 to 25°C and the relative humidity at 40% to 50% with 12 h dark and 12 h light cycle. The animals were provided with clean drinking water and commercial food. The animal cages were cleaned every three days until the end of the experiment.

After a week of acclimation, the animals were randomly divided into four groups based on the dosage of ZnO NPs: 0 (control group), 50, 150 and 450 mg/kg; there were 10 mice in each group. Based on Talebi's study, the lowest dose used in this study was 50 mg/kg, while the 150 and 450 mg/kg were set in a threefold gradient.<sup>19</sup> The

ZnO NPs in powder form were weighed and mixed with 2 mL saline. The mixture was subjected to ultrasonication for 30 mins and vortexed for 1 min before use. The mice in the experimental group were administered with 50, 150 and 450 mg/kg ZnO NPs for 14 days by gavage. Correspondingly, the control group was treated with the same volume of saline. The body weight and clinical symptoms of the mice were recorded daily during the 14-day experiment. Twenty-four hours after the last gavage, all mice were anesthetized, and the blood samples were collected by eyeball extraction immediately after sacrifice by cervical dislocation. The mice were dissected and the organs were collected, weighed, and visually analyzed. Both the serum and tissue samples were stored in a freezer at  $-80^{\circ}\text{C}$  until use.

### Salubrinal Supplementation

Fifteen male Kunming mice (7 weeks old, weight  $32 \pm 2$  g) were randomly divided into three groups: the control, 450 mg/kg and 450 mg/kg with 1.5 mg/kg salubrinal (sal) ( $n=5$ ) treatment groups. One group of mice was treated with saline and the other with 450 mg/kg ZnO NPs by gavage. The remaining group was treated with 1.5 mg/kg salubrinal (MedChemExpress, USA) by intraperitoneal injection at 30 mins after exposure to 450 mg/kg ZnO NPs. For 14 consecutive days, the clinical symptoms were observed and recorded daily. Finally, all mice were dissected and the organs were collected, weighed, and visually analyzed. Both the serum and tissue samples were stored in a freezer at  $-80^{\circ}\text{C}$  for future use.

### Sperm Counts

The assessment of testicular sperm count and evaluation was adopted from the studies reported by Kisin et al<sup>29</sup>. The left epididymis was separated from the testis, and the attached adipose tissue was carefully removed. The collected epididymis was fully minced and its tail was squeezed before it was placed in 1 mL of normal saline to release the sperm. It was incubated in a  $37^{\circ}\text{C}$  water bath for 15 mins. A 200  $\mu\text{L}$  aliquot of the sperm suspension was added to 1 mL of  $90^{\circ}\text{C}$  saline to kill the sperm. A 10  $\mu\text{L}$  sample was transferred into a hemocytometer that was placed under an optical microscope to determine the sperm count (Nikon eclipse Ti). Another 20  $\mu\text{L}$  of the sperm suspension was applied on a microscope glass slide to which 3 mL of 10% formaldehyde and 2 mL of 1% eosin were added. This was incubated at room temperature for 30 mins before the quality of the

sperms was evaluated. All studies were performed in triplicate.

### Histopathology

The testes were evaluated for the histopathological lesions of exposure to ZnO NPs. The testes were preserved with 4% paraformaldehyde upon extraction from the mice. Aliquots were dehydrated with different gradients of ethanol before these were embedded in paraffin. The paraffin block was sectioned at 5  $\mu\text{m}$  thickness and stained with hematoxylin and eosin. The stained sections were fixed on the slides, and the seminiferous tubules, lumens and germ cells were observed at  $200\times$  and  $400\times$  magnifications under an optical microscope.

### Assay for Testosterone in Serum

The effects of ZnO NPs exposure over 14 days on the testosterone levels in serum were evaluated. Whole blood samples were stored at  $4^{\circ}\text{C}$  for 6 hrs and centrifuged at 4000 r/min for 10 mins before the supernatant was isolated for the testosterone assay. Serum samples were collected to evaluate the level of the male sex hormone testosterone using Cayman chemical's Testosterone ELISA kit (Item No. 582701) according to the manufacturer's protocol. Absorbance was recorded at 405 nm with a microplate reader (Thermo Scientific, USA). The testosterone levels were obtained using the established standard curve from the ELISA kit.

### Total Zinc Determination in Testis and Epididymis

The frozen right testis and the epididymis were thawed and processed as follows: weighed samples of 0.2–0.4 g tissues were treated with 10 mL of 65%  $\text{HNO}_3$  and 2 mL of 70%  $\text{HClO}_4$  and heated on an electric heating board to  $230^{\circ}\text{C}$  at which point the digested solution became clear. This was further heated gradually to  $280^{\circ}\text{C}$  down to 0.5 mL until the liquified tissues became clear and transparent, which indicated that the digestion was complete. This liquid was cooled down to ambient temperature and diluted to 25 mL with ultrapure water before it was used to establish the zinc concentration by atomic absorption spectroscopy (AAS) (TAS-990, Purkinje General Instrument Co., China). Before analysis, the AAS was calibrated by running six standard concentrations (0, 0.1, 0.2, 0.3, 0.4 and 0.5  $\mu\text{g}/\text{mL}$ ) of zinc.

## RNA Isolation and Quantitative Real-Time PCR

Total RNA in the testis was extracted with Axyprep™ Multisource Total RNA Miniprep Kit (Axygen) following the instruction manual. This was reverse-transcribed to make cDNA using a reverse transcription mixture (Takara Bio Inc.). The primers were designed with Primer Express Software (Applied Biosystems, Foster City, CA, USA) and Oligo Primer Analysis Software version 6.0 (Molecular Biology Insights, Inc.; DBA Oligo, Inc.).

The template DNA strand was mixed with the primer and TB Green (Takara Bio Inc.; Cat. #:RR820A). Real-time qPCR was operated on ABI 7900HT Fast Real-Time System (Applied Biosystems, Foster City, CA) under the following conditions: 40 cycles of 95°C for 30 s, 95°C for 5 s, 60°C for 1 min. Relative quantification of mRNA was calculated using the  $2^{-\Delta\Delta Ct}$  method. The internal reference gene was *GAPDH*.

## Immunofluorescence Assay

The JNK and caspase-12 expression levels in the testis were evaluated with immunofluorescence assay. All procedures were based on A Guide to Successful Immunofluorescence from Cell Signaling Technology, Inc. The mean pixel fluorescence intensity was analyzed by ImageJ 6.0 (National Institutes of Health).

## Statistical Analysis

All reported data shown were the mean  $\pm$  SD of triplicate measurements that were analyzed using the SPSS (version

22) software. One-way ANOVA was used for statistical significance between groups. The differences were considered significant at  $P < 0.05$  indicating \*,  $P < 0.01$  indicating \*\*, and  $P < 0.001$  indicating \*\*\*.

## Results

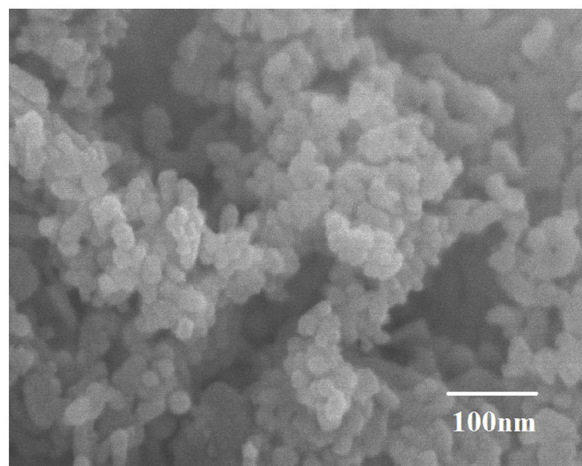
### Characterization of ZnO NPs

It is important to establish the shape and size of the NPs because these physical characteristics affect the stability, cell damage, and penetration abilities of the particles. The observations under the SEM indicated that the ZnO NPs were spherical in geometry with an average diameter of 30 nm (Figure 1A and B). The shape of the nanoparticles indicated that there were no sharp edges that could stab the cells or the tissues. The size was small enough in order for the NPs to be assimilated very easily by cells in the mice which had an average size at least 2 orders of magnitude bigger than the ZnO NPs.<sup>30</sup>

### Body and Testicular Weights and Zinc Accumulation

Changes in the body and testicular weights, as well as zinc accumulation in the testis and epididymis, were evaluated as possible indicators of ZnO NPs toxicity. The net increase in body weight and the organ index of testis and epididymis were calculated as shown in Table 1. The weight gain of the mice in the experimental group that were subjected to a 14-day oral administration of the ZnO NPs was significantly decreased. However, testicular organ

A



B

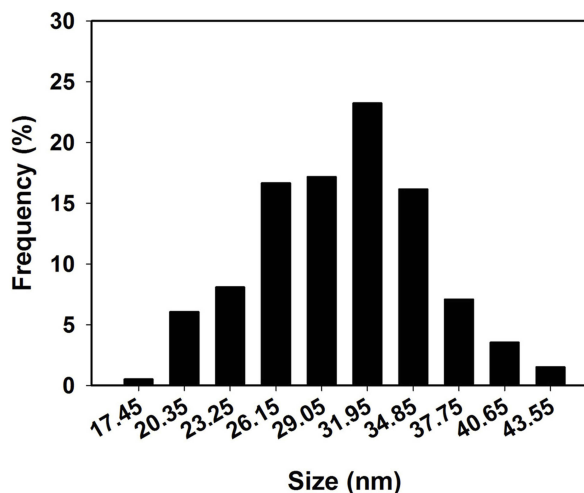


**Figure 1** Characterization of ZnO NPs. (A) SEM image and (B) the size distribution of ZnO NPs.



**Table 1** Changes in Body Weight and Relative Testis and Epididymis Weight at Necropsy

Group	Control	50 mg/kg	150 mg/kg	450 mg/kg
Net increase of body weight (g)	3.83 ±0.49	2.95 ±0.58	2.56 ±1.13	2.23 ±0.27*
Relative testicular weight (mg/g)	5.61 ±0.38	6.02 ±0.09	6.52 ±0.15*	6.53 ±0.63
Relative epididymis weight (mg/g)	1.06 ±0.26	1.56 ±0.02*	1.1±0.05	1.60 ±0.09*

**Notes:** Relative organ weight = organ weight (mg)/body weight (g), \*P<0.05 compared with control.

index increased with dose more significantly in the 150 mg/kg ZnO NPs treatment group, while the organ index for the epididymis significantly increased in the 50 and 450 mg/kg ZnO NPs treatment groups. In addition, the Zn content in the testis and epididymis was higher in the epididymis of the 50 and 450 mg/kg ZnO NPs groups (Figure 2D and E).

## Histopathological Evaluation

The control group exhibited normal histopathology of the testis and other related tissues. The seminiferous tubules were closely connected and arranged neatly; the germ cells were abundant and spermatogonia, spermatocyte and spermatid were normal (Figure 2A-a, e). Unlike the control, the 50 mg/kg treatment group showed the seminiferous tubules as segregated, the germ cell layer was random and the sperm in the lumen was low in number (Figure 2A-b, f). In the 150 mg/kg group, the seminiferous tubules were degenerated with larger distances, and there was significant vacuolization of the Sertoli cells (Figure 2A-c, g). More significant difference with the control group was seen in the 450 mg/kg treatment group because the seminiferous tube was absent, the various germ cells were all low in number, the spermatogenic cells were degenerated and necrotic with signs of shedding (Figure 2A-d, h) and inter-tubular edema and Leydig cell vacuolization was observed. All of these were indicative of damage caused by the treatment with 450 mg/kg ZnO NPs over the timeframe of the study.

## Sperm Counts

Aside from the histopathological evaluation of the testis and related tissues, sperm count was used as an indicator of the reproductive toxicity of the ZnO NPs. The 50 mg/kg ZnO NPs treatment group showed no significant difference

in the sperm count from the left epididymis compared with the control group. However, the 150 mg/kg (P<0.01) and the 450 mg/kg (P<0.001) groups exhibited a significant decrease in sperm counts (Figure 2B).

## Testosterone Levels in Serum

The change in the level of testosterone in male mice serum was recorded and is shown in Figure 2C. The results indicated that the higher the dosage of the ZnO NPs, the lower the level of testosterone in the serum compared with the control group. The results indicated that higher dosages of ZnO NPs resulted in more and/or bigger lesions or complete degeneration of testes cells (Figure 2A), the function of which has been primarily to produce sperms and testosterone in males.

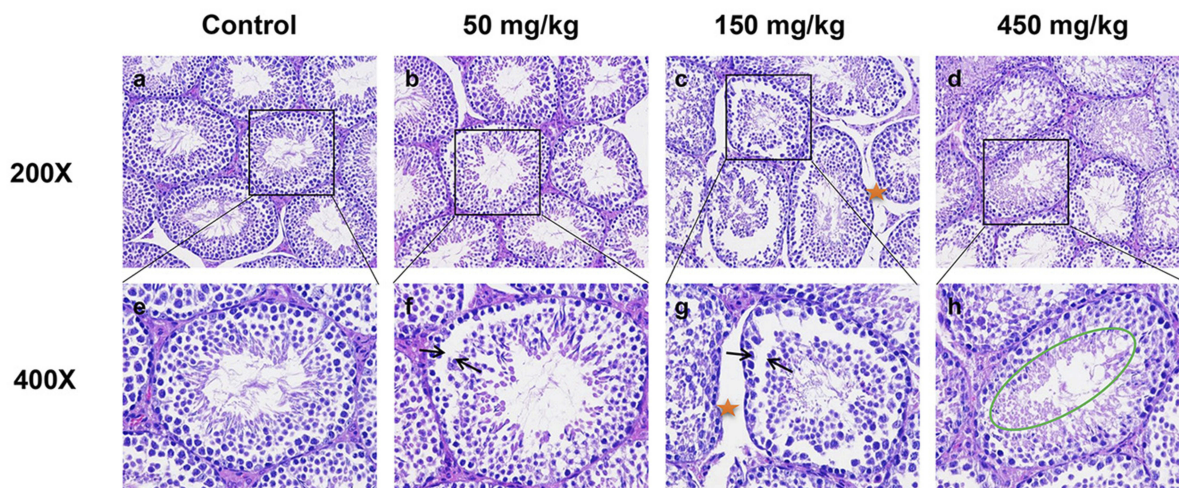
## The Level of Relative Gene Expression in Testis

In this study, RT-qPCR was used to analyze the gene expressions related to ER stress, apoptosis and testosterone production. The results showed that the unfolded protein responsive protein immunoglobulin-binding protein (*BIP*) and the X-box-binding protein 1 splicing (*XBPIs*) were significantly up-regulated in the group treated with 450 mg/kg ZnO NPs; the ER stress-associated gene inositol-requiring protein 1 $\alpha$  (*IRE1 $\alpha$* ) was up-regulated in the experimental groups; Jun kinase (*JNK*) and the transcription of CCAAT/enhancer-binding protein (C/EBP) homologous protein (*CHOP*) expression were up-regulated in 150 mg/kg ZnO NPs and 450 mg/kg ZnO NPs treatment groups. In addition, the ratio of Bcl-2-associated X protein (*Bax*) and B cell lymphoma-2 (*Bcl-2*) was significantly increased compared with the control group. The caspase-12 and caspase-3 in the caspase family that are involved in the apoptotic signaling pathway were up-regulated. Some important enzymes in the testosterone synthesis pathway, steroidogenic acute regulatory protein (*StAR*) were down-regulated significantly in the 450 mg/kg group while cytochrome *P450 $\text{scc}$*  showed no significant alteration (Figure 3).

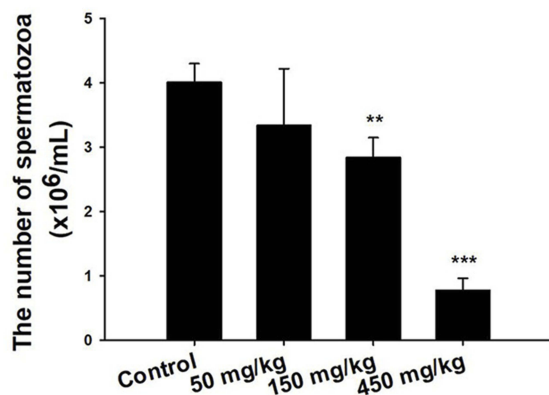
## Effects of ER-Stress Inhibitor Salubrinal After Treatment with ZnO NPs

The effect of an ER-stress inhibitor, sal was used to evaluate further the mechanism of the ZnO NPs toxicity in male mice. Sal, which has been known to inhibit ER stress, was administered to the group of male mice that were previously treated with 450 mg/kg ZnO NPs. In the presence of sal, the

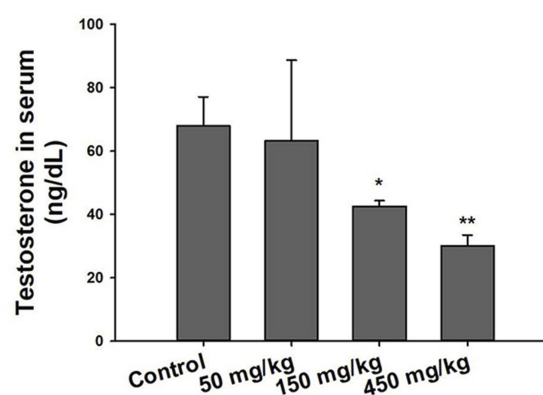
A



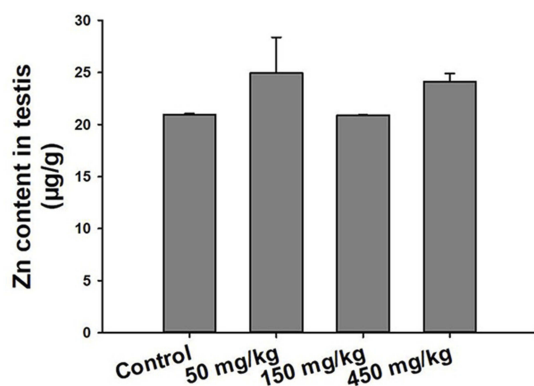
B



C



D



E

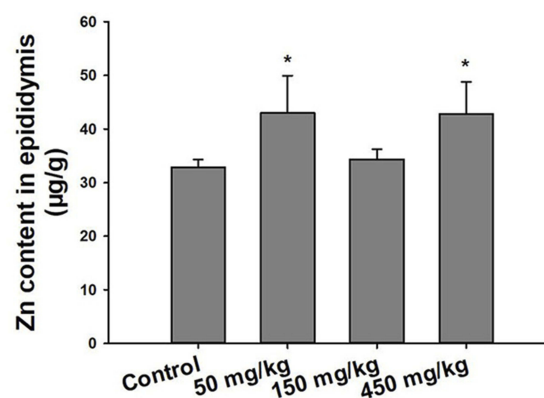


**Figure 2** Histopathology, sperm count, testosterone levels, and AAS for Zn. **(A)** Light microscopy of cross-sections of H&E stained testes from male mice. Arrow indicates a lesion in seminiferous tubule; pentastar indicates the vacuolization of Sertoli cells; green circle indicates disorder in germ cell. **(B)** Sperm count in the left epididymis. The data in sperm per milliliter of saline. **(C)** Testosterone concentration in serum detected by ELISA. **(D)** and **(E)** Concentration of Zn in testes and epididymis. Data are expressed as mean  $\pm$  SD, \* $P$ <0.05, \*\* $P$ <0.01, \*\*\* $P$ <0.001 compared with control.

results showed no significant histopathological lesions in the testicular cells (Figure 4A) even though the Zn contents

in the testis and epididymis were similar with those without sal treatment (Figure 4E and F). In addition, the number of

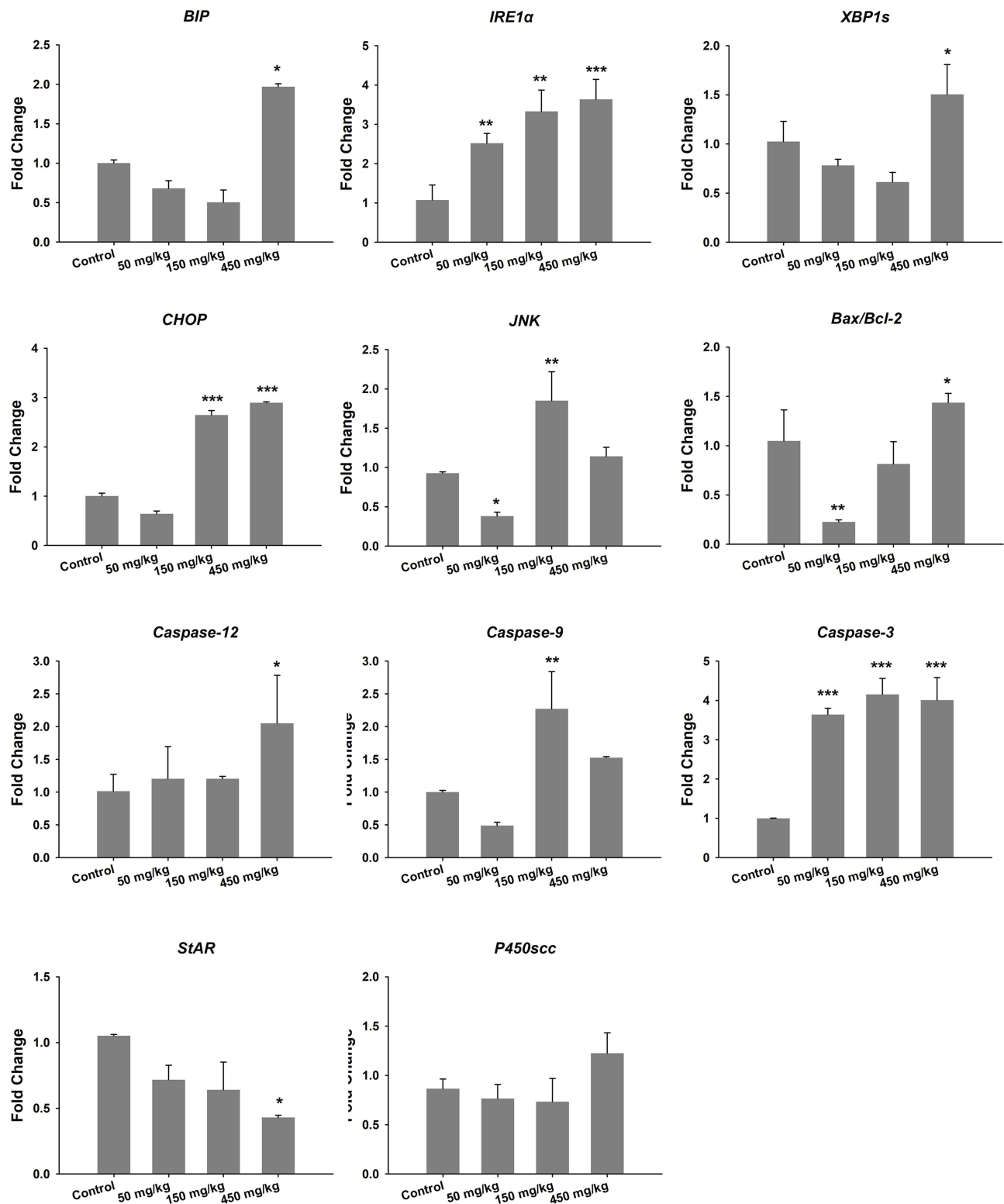


**Figure 3** Gene expression of ER stress, apoptosis and testosterone production in testis. \* $P < 0.05$ , \*\* $P < 0.01$ , \*\*\* $P < 0.001$  compared with control.

spermatozoa and testosterone in the sal-treated group was significantly elevated relative to the 450 mg/kg group that was not administered with sal (Figure 4B and D).

Furthermore, the sal-treated experimental group showed that the mRNA levels of related genes were similar to the control group except for *StAR* (Figure 4C). The

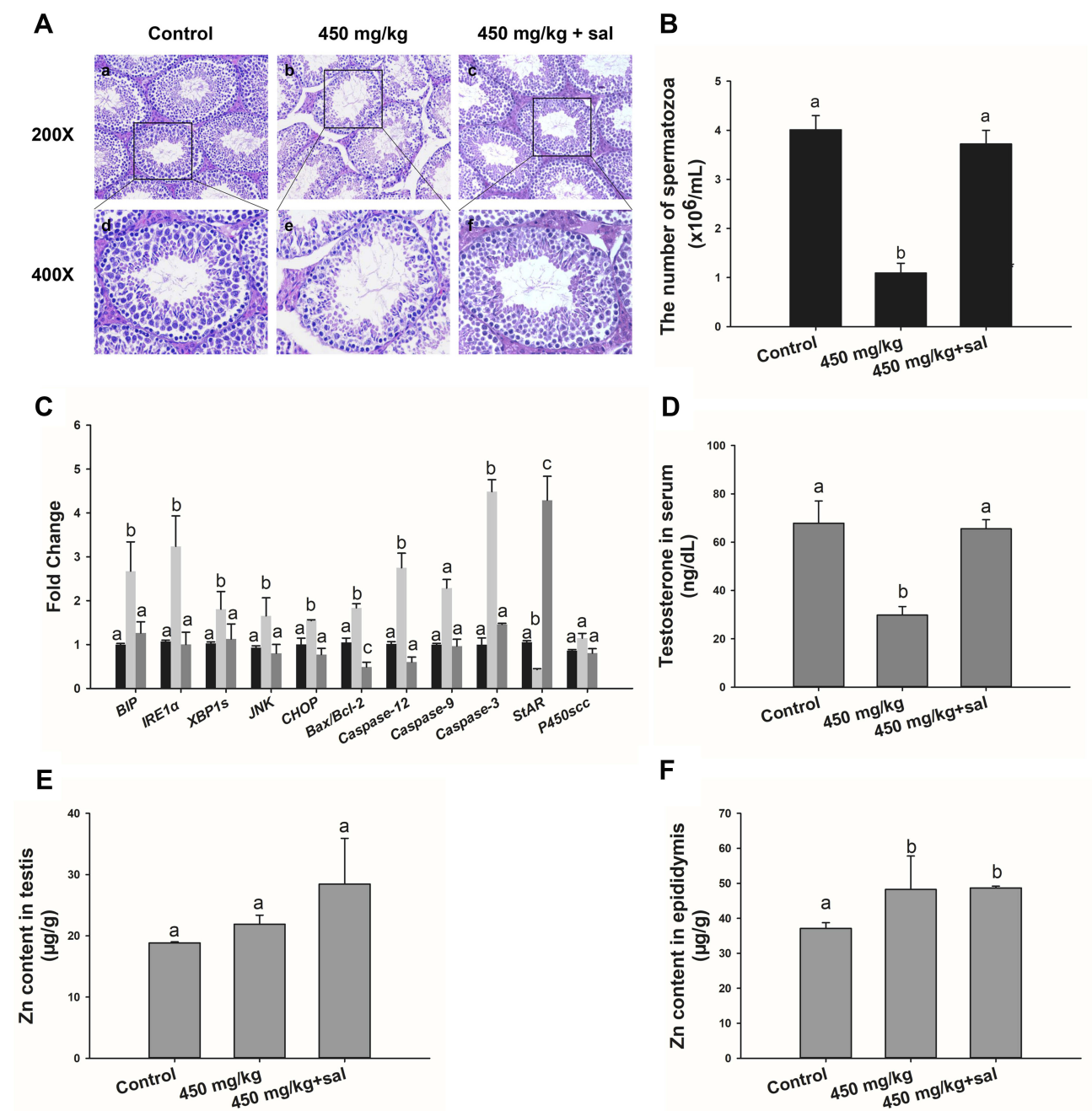


**Figure 4** Effect of sal treatment in 450 mg/kg ZnO NPs group. **(A)** Light microscopy of cross-sections of H&E stained testis. **(B)** Number of sperms in the left epididymis. The data are in sperm per milliliter of saline. **(C)** Gene expression levels of ER stress, apoptosis and testosterone in testis. **(D)** Testosterone concentration in serum detected by ELISA. **(E)** and **(F)** Concentration of Zn in testes and epididymis. Data are expressed as mean  $\pm$  SD. Bars that do not share any letters (a, b, c) are significantly different ( $P < 0.05$ ).

quantification of immunofluorescence from caspase-12 and JNK was significantly decreased compared with the 450 mg/kg group that was not treated with sal (Figure 5).

## Discussion

Among the nanoparticles, ZnO NPs have been extensively utilized in various types of consumer products. Thus, the goal of this study was to evaluate the potential

reproductive risks in males exposed by gavage to various doses of ZnO NPs that are spherical with an average diameter of 30 nm.

The weight gain in the animals was the fastest to evaluate among the parameters taken into consideration in this study. The results indicated that the weight gain decreased with an increased dosage of ZnO NPs (Table 1). These observations were similar to those reported by Hong et al



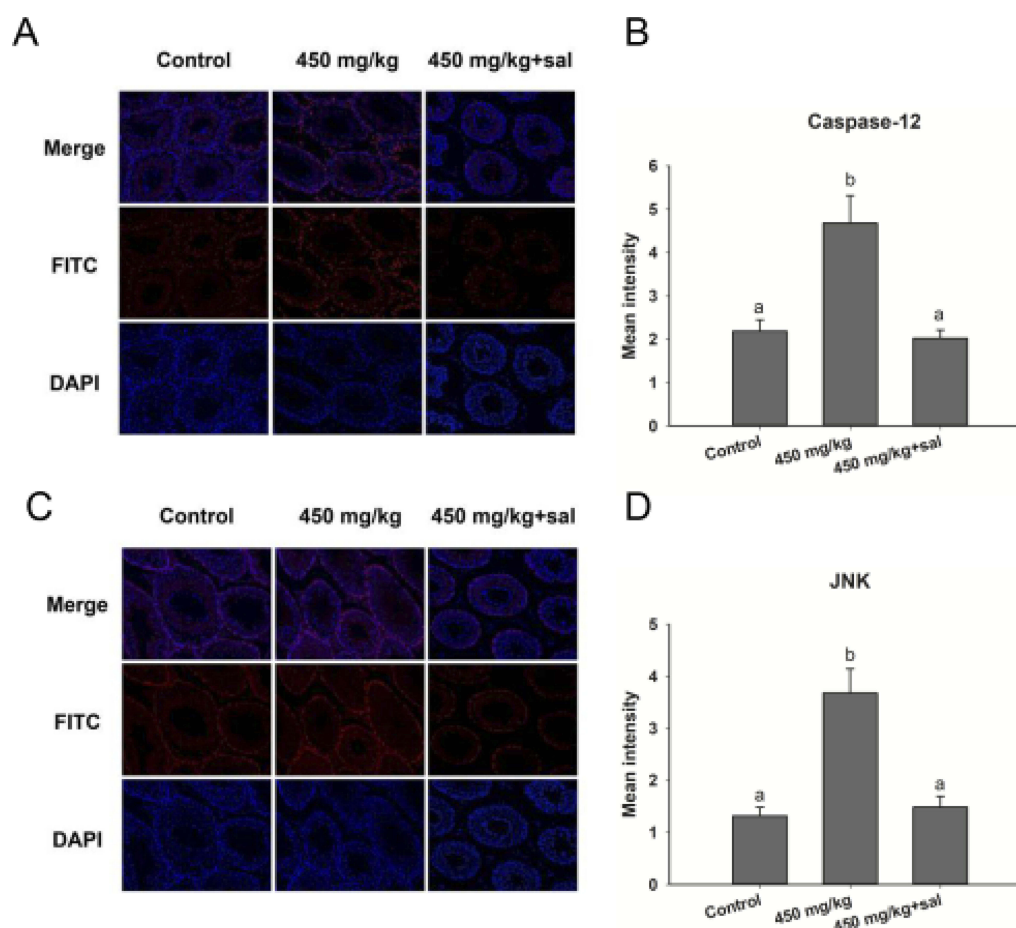


**Figure 5** Immunofluorescence detection of caspase-12 and JNK in the testis of mice treated with ZnO NPs and salubrinal. (A) Caspase-12; (C) JNK. Blue: DAPI; Red: JNK and caspase-12. Magnification: 200 $\times$ . (B and D) The panels are semi-quantitative analysis. Data are expressed as mean  $\pm$  SD.

when they administered different doses (0, 500, 1000, 2000 mg/kg/d) of 100 nm ZnO NPs for 16 days in SD rats.<sup>31</sup>

Evaluation of the level of Zn in the testis was used as a possible indicator of 30 nm ZnO NPs penetration of the blood-testis barrier. The results indicated a higher level of Zn in the epididymis of the experimental groups compared with the control, especially those treated with the 50 and 450 mg/kg ZnO NPs (Figure 2E). However, in the testis, the difference in the level of Zn between the control and the experimental groups was not as pronounced (Figure 2D). Therefore, we changed the mind based on the Zn level. It was possible that the ZnO NPs reproductive toxicity could be partially due to systemic and multi-organ impact. It was also possible that the ZnO NPs could enter in the male reproductive system and disrupt the endocrine system<sup>32</sup> that led to the reproductive toxicity of ZnO NPs, but this was not the focus of our research at this time.

It has been reported that the accumulation of nanoparticles contributed to deleterious effects in the testis,

including testicular lesions, sperm malformations, alterations in serum sex hormone levels and testis-specific gene expressions.<sup>31,33,34</sup> Taking these reports into consideration, the spermatogenesis was evaluated and the results indicated that the number of sperms decreased in a dose-dependent manner with the highest being at 450 mg/kg group which exhibited almost a 75% decrease compared with the control (Figure 2B). This decrease in sperm may be the result of the histopathological studies which showed a thinner spermatogenic epithelium, possible Sertoli cell apoptosis, and vacuolization in the spermatogenic tubules that were indicative of Leydig cells necrosis (Figure 2A). Similar studies also found that ZnO NPs led to testicular histopathological changes, which caused destructive effects on spermatogenesis.<sup>17</sup> Han et al demonstrated that in vitro ZnO NPs could be absorbed by Leydig cells and Sertoli cells that increased reactive oxygen species (ROS) which led to apoptosis.<sup>8</sup> Harmful effects on the testicular Leydig cells could decrease the production of testosterone,

a hormone that is necessary for spermatogenesis. In this study, testosterone concentration decreased with an increased dose of ZnO NPs (Figure 2C) which could suppress spermatogenesis.<sup>35</sup> Hence, a negative impact of ZnO NPs to the Leydig cells which are responsible for 80% of the testosterone production could induce a reproductive decline in male mice.

The mechanism of ZnO NPs toxicity was evaluated based on indications that ZnO NPs could generate ROS that activate ER stress.<sup>36</sup> Therefore, we hypothesized that ER stress could cause ZnO NP-induced male reproductive toxicity. BIP, also known as glucose-regulated protein, that is 78 kDa (GRP78), has also been known as a marker for activating ER stress.<sup>37,38</sup> When BIP gets separated from IRE1 $\alpha$ , this IRE1 $\alpha$  gets phosphorylated into active endonuclease which could selectively excise 26nt intron from XBP1 mRNA that could be converted to the transcription factor box binding protein 1 splicing (XBPs). When this happens, the XBPs penetrates the nucleus to enhance the expression of ER chaperones like CHOP, BIP and proteins related to ER-associated degradation (ERAD) that accelerate protein folding and misfolded protein degradation to alleviate unfolded protein response (UPR).<sup>39</sup> In this study, the ZnO NPs induced up-regulation of the ER-stress genes IRE1 $\alpha$ , XBPs, BIP, and CHOP in mice testis (Figure 3). Similarly, Chen et al found that the IRE1 $\alpha$ /XBPs pathways were fully activated in the human umbilical vein endothelial cells in the presence of ZnO NPs.<sup>36</sup> Although the activation of ER stress could restore homeostasis, long-term ER stress led to the relevant apoptosis pathway.<sup>25</sup> It was reported that IRE1 $\alpha$  could activate caspase-12 which in turn mediated the pre-apoptotic signaling pathway by activating caspase-9 and caspase-3 to induce apoptosis.<sup>40</sup> In another mechanism study, IRE1 $\alpha$  was found essential for the JNK signal transduction pathway in response to ER stress.<sup>41</sup> JNK, similar to CHOP, could inhibit anti-apoptotic Bcl-2 to break the balance between the expression levels of the proteins Bax and Bcl-2, which could mediate the mitochondrial apoptotic mechanism that could activate caspase-9.<sup>42</sup> In another study, caspase-3, as a downstream target of caspase-9, was activated which led to apoptosis.<sup>43</sup> In the present study, as shown in Figure 3, JNK was up-regulated in the presence of 150 mg/kg ZnO NPs, and the expression of CHOP was also significantly increased in both the 150 and 450 mg/kg, and the ratio of Bax/Bcl-2 increased in the 450 mg/kg ZnO NPs. These results could be taken as indicators of possible activation of mitochondrial-mediated apoptosis. Consistent with findings in this research, Wang's study found that ZnO NPs led to

apoptosis by activating JNK and Bax/Bcl-2-dependent mitochondrial apoptotic mechanism in an in vitro study.<sup>44</sup> In this present in vivo study, the results showed that ZnO NPs induced the up-regulation of caspase-12 in 450 mg/kg treatment group, and caspase-9 was up-regulated in the 150 mg/kg treatment group. The expression of caspase-3 was significantly increased in all the treatment groups which could be another indication of the activation of apoptosis.<sup>43</sup> Moreover, the immunofluorescence analysis supported the caspase-12 results (Figure 6A and C), and the JNK (Figure 6B and D) levels were more significantly expressed in the testes of the treatment groups. In addition, when ER-stress inhibitor salubrinal was applied to further demonstrate the activation of ER stress in ZnO NP-induced reproductive toxicity, the sal-treated mice showed no lesions in the testis and most of the ER stress-related genes significantly decreased, especially IRE1 $\alpha$ , CHOP and caspase-3 (Figure 4C). The same was observed in the immunofluorescence analysis, which indicated that the toxicity of ZnO NPs was significantly attenuated in the presence of the ER-stress inhibitor. The results indicated that ER stress in the presence of 30 nm ZnO NPs may have induced testicular germ cell apoptosis as well as mitochondrial-dependent apoptosis (Figure 7), which was not observed when the ZnO NPs treated mice were subsequently treated with sal.

Germ cell apoptosis could affect normal testicular function in the same manner that Sertoli cell apoptosis could prevent spermatogenesis.<sup>45</sup> Additionally, reports also indicated that testosterone production could be inhibited by Leydig cells apoptosis.<sup>46,47</sup> The regulation of testosterone synthase and protein expression was affected by multiple transcription factors at the transcriptional level according to a study.<sup>48</sup> In the complex testosterone synthetic pathway, reports indicated that StAR was responsible for the transport of hydrophobic low-density cholesterol from the cytosol to the mitochondrial inner membrane, which is a key step in testosterone synthesis.<sup>49</sup> The cytochrome P450 enzymes had been shown to convert cholesterol to pregnenolone.<sup>50,51</sup> Hence, the effects of toxic materials on the mRNA levels of *StAR* and *P450scc* could be used as indicators of possible toxicity. In this study, RT-qPCR results showed a significant down-regulation of *StAR*, while the transcriptional level of *P450scc* had no statistical difference between the control and the treated groups (Figure 3). Interestingly, eliminating the activation of ER stress up-regulated *StAR* dramatically, while testosterone level in serum was similar with the control.

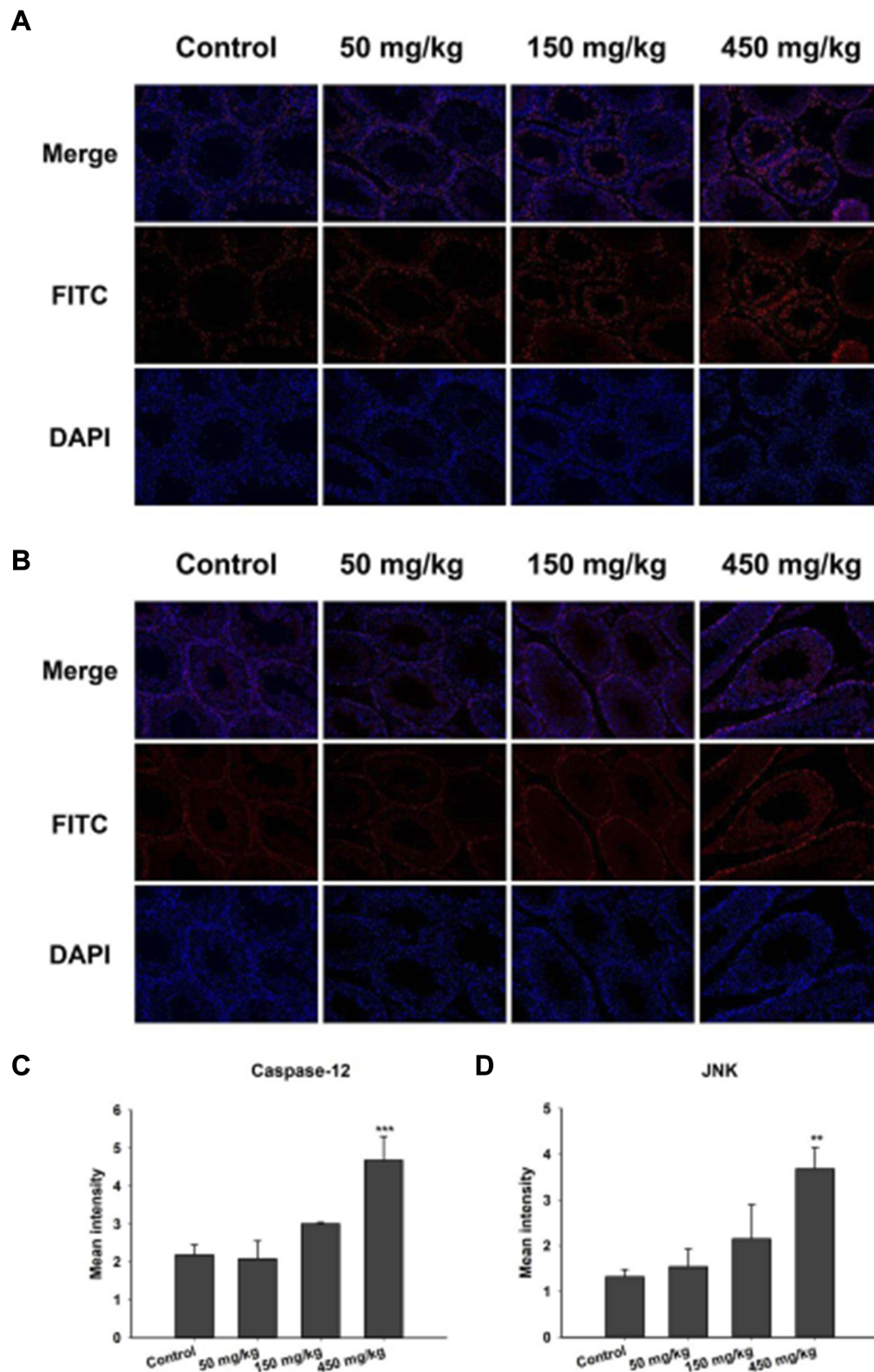


**Figure 6** Immunofluorescence detection of caspase-12 and JNK in testis tissue. **(A)** Caspase-12; **(B)** JNK. Blue: DAPI; Red: JNK and caspase-12. Magnification: 200 $\times$ . **(C and D)** The panels are semiquantitative analysis (mean  $\pm$  SD), \*\* $P < 0.01$ , \*\*\* $P < 0.001$  compared with control.



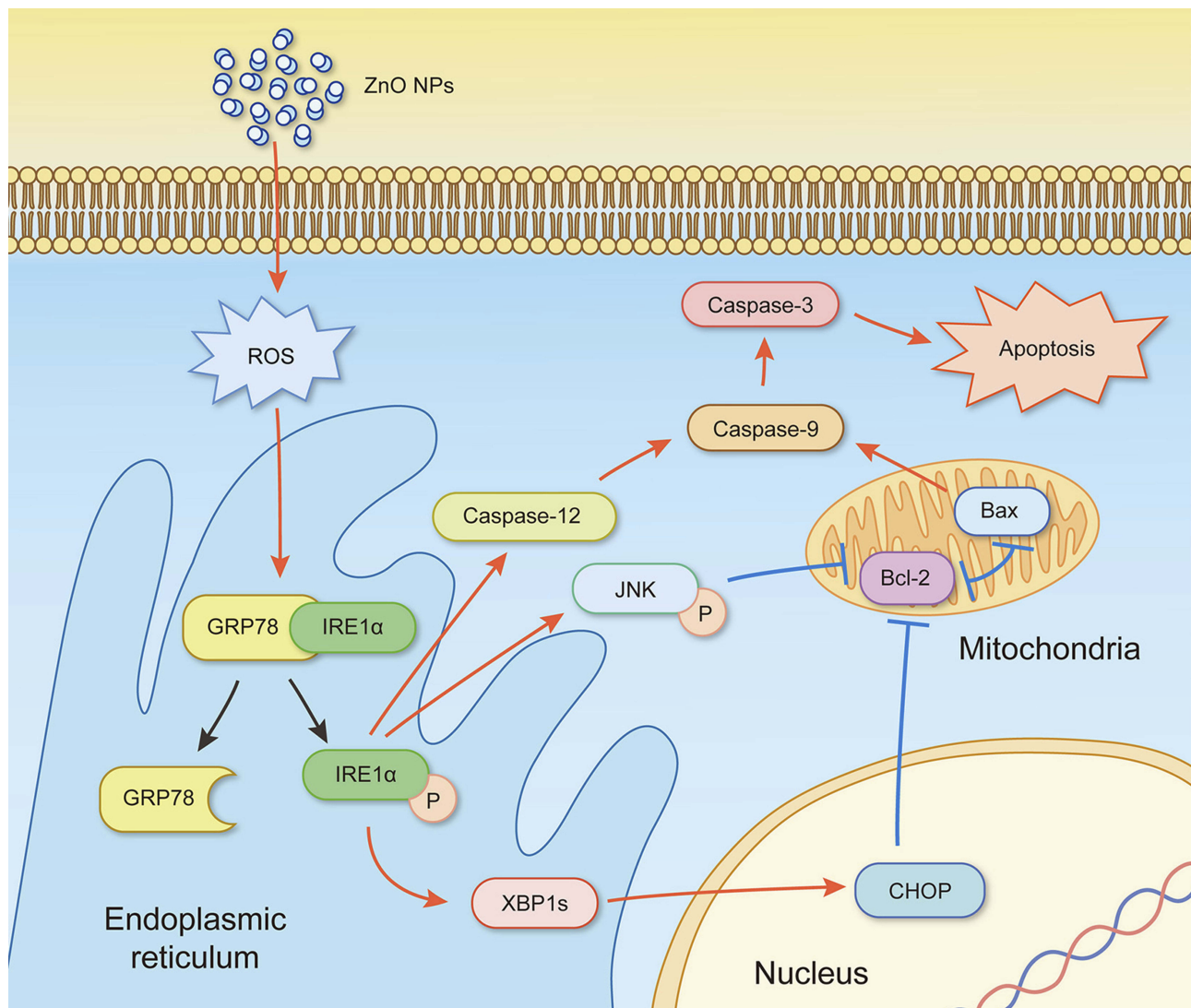


**Figure 7** Schematic diagram for the activation of ER-stress pathway in testis of ZnO NPs-male mice. Simultaneous mitochondrial apoptosis caused imbalance in the Bax/Bcl-2 signaling. “↑” activation, “⊥” inactivation, “P” phosphorylation and “⊥” antagonism.

Based on these observations, it could be inferred that the apoptosis of the Leydig cells in the presence of the ZnO NPs affected testosterone production through the down-regulation of *StAR*.

## Conclusion

In this study, the effects of oral administration of spherical 30 nm diameter ZnO NPs for 14 days in male reproduction were investigated. The results indicated that exposure to  $\geq 50$  mg/kg doses of ZnO NPs caused testicular damages, spermatogenesis abnormalities and decreased testosterone levels in the serum. The damages in the seminiferous tube, vacuolization of Sertoli and Leydig cells, and low germ cell counts were more significant in the higher dosage of ZnO NPs. Sperm cell

counts were also lower at higher ZnO NPs dosage. All these observations indicated possible ZnO NPs toxicity in the male reproductive system.

In terms of the underlying mechanism of toxicity, the ZnO NPs exhibited up-regulation of the gene expressions for ER stress such as the IRE1 $\alpha$ , XBP1s, BIP, CHOP. The expression of caspase-3 was significantly increased in all the treatment groups which reflected the activation of apoptosis. In addition, RT-qPCR also showed significant down-regulation of the gene *StAR*, which has been accepted as a key player in testosterone synthesis. Therefore, it was very likely that apoptosis and ER stress contributed to ZnO NPs induced down-regulation of genes for testosterone production which led to a significant decrease in testosterone levels. When an ER-stress inhibitor salubrinal was administered to the 450 mg/kg



ZnO NPs treatment group, the damages to the seminiferous tube and vacuolization of Sertoli and Leydig cells were not observed. Furthermore, the testosterone levels in the serum were similar to the control group. Thus, it may be inferred that the ZnO NPs reproductive toxicity in male mice occurred via apoptosis and ER-stress signaling pathway.

## Acknowledgment

This work was supported by the National Natural Science Foundation of China (81771658 and 81560537).

## Disclosure

Zoraida P Aguilar is employed by Zystein, LLC., Fayetteville, AR, USA. The authors report no other conflicts of interest in this work.

## References

- Peters RJ, Bouwmeester H, Gottardo S, et al. Nanomaterials for products and application in agriculture, feed and food. *Trends Food Sci Tech.* 2016;54:155–164.
- Diez-Pascual AM, Diez-Vicente AL. ZnO-reinforced poly (3-hydroxybutyrate-co-3-hydroxyvalerate) bionanocomposites with antimicrobial function for food packaging. *ACS Appl Mater Interfaces.* 2014;6(12):9822–9834. doi:10.1021/am502261e
- Shi L-E, Li Z-H, Zheng W, Zhao Y-F, Jin Y-F, Tang Z-X. Synthesis, antibacterial activity, antibacterial mechanism and food applications of ZnO nanoparticles: a review. *Food Addit Contam Part A.* 2014;31(2):173–186. doi:10.1080/19440049.2013.865147
- Liu R, Lal R. Potentials of engineered nanoparticles as fertilizers for increasing agronomic productions. *Sci Total Environ.* 2015;514:131–139. doi:10.1016/j.scitotenv.2015.01.104
- Liu Y, Nie Y, Wang J, et al. Mechanisms involved in the impact of engineered nanomaterials on the joint toxicity with environmental pollutants. *Ecotoxicol Environ Saf.* 2018;162:92–102. doi:10.1016/j.ecoenv.2018.06.079
- Wang C, Lu J, Zhou L, et al. Effects of long-term exposure to zinc oxide nanoparticles on development, zinc metabolism and biodistribution of minerals (Zn, Fe, Cu, Mn) in mice. *PLoS One.* 2016;11(10):e0164434. doi:10.1371/journal.pone.0164434
- Gilbert B, Fakra SC, Xia T, Pokhrel S, Mädler L, Nel AE. The fate of ZnO nanoparticles administered to human bronchial epithelial cells. *ACS Nano.* 2012;6(6):4921–4930. doi:10.1021/nn300425a
- Han Z, Yan Q, Ge W, et al. Cytotoxic effects of ZnO nanoparticles on mouse testicular cells. *Int J Nanomedicine.* 2016;11:5187. doi:10.2147/IJN.S111447
- Chen P, Wang H, He M, Chen B, Yang B, Hu B. Size-dependent cytotoxicity study of ZnO nanoparticles in HepG2 cells. *Ecotoxicol Environ Saf.* 2019;171:337–346. doi:10.1016/j.ecoenv.2018.12.096
- Liu Q, Xu C, Ji G, et al. Sublethal effects of zinc oxide nanoparticles on male reproductive cells. *Toxicol in Vitro.* 2016;35:131–138. doi:10.1016/j.tiv.2016.05.017
- Esmaeillou M, Moharamnejad M, Hsankhani R, Tehrani AA, Maadi H. Toxicity of ZnO nanoparticles in healthy adult mice. *Environ Toxicol Pharmacol.* 2013;35(1):67–71. doi:10.1016/j.etap.2012.11.003
- Park H-S, Shin -S-S, Meang EH, et al. A 90-day study of subchronic oral toxicity of 20 nm, negatively charged zinc oxide nanoparticles in sprague dawley rats. *Int J Nanomedicine.* 2014;9(Suppl 2):79.
- Inhorn MC, Patrizio P. Infertility around the globe: new thinking on gender, reproductive technologies and global movements in the 21st century. *Hum Reprod Update.* 2015;21(4):411–426. doi:10.1093/humupd/dmv016
- Bisht S, Faiq M, Tolahunase M, Dada R. Oxidative stress and male infertility. *Nat Rev Urol.* 2017;14(8):470–485. doi:10.1038/nrurol.2017.69
- Lan Z, Yang W-X. Nanoparticles and spermatogenesis: how do nanoparticles affect spermatogenesis and penetrate the blood–testis barrier. *Nanomedicine.* 2012;7(4):579–596. doi:10.2217/nnm.12.20
- Yoshida S, Hiyoshi K, Ichinose T, et al. Effect of nanoparticles on the male reproductive system of mice. *Int J Androl.* 2009;32(4):337–342. doi:10.1111/ija.2009.32.issue-4
- Mozaffari Z, Parivar K, Roodbari NH, Irani S. Histopathological evaluation of the toxic effects of zinc oxide (ZnO) nanoparticles on testicular tissue of NMRI adult mice. *Adv Stud Biol.* 2015;7:275–291. doi:10.12988/asb.2015.5425
- Abbasalipourkabar R, Moradi H, Zarei S, et al. Toxicity of zinc oxide nanoparticles on adult male Wistar rats. *Food Chem Toxicol.* 2015;84:154–160. doi:10.1016/j.fct.2015.08.019
- Talebi AR, Khorsandi L, Moridian M. The effect of zinc oxide nanoparticles on mouse spermatogenesis. *J Assist Reprod Genet.* 2013;30(9):1203–1209. doi:10.1007/s10815-013-0078-y
- Saliani M, Jalal R, Goharshadi E. Mechanism of oxidative stress involved in the toxicity of ZnO nanoparticles against eukaryotic cells. *Nanomed J.* 2016;3(1):1–14.
- Song W, Zhang J, Guo J, et al. Role of the dissolved zinc ion and reactive oxygen species in cytotoxicity of ZnO nanoparticles. *Toxicol Lett.* 2010;199(3):389–397. doi:10.1016/j.toxlet.2010.10.003
- Brodsky JL, Skach WR. Protein folding and quality control in the endoplasmic reticulum: recent lessons from yeast and mammalian cell systems. *Curr Opin Cell Biol.* 2011;23(4):464–475. doi:10.1016/j.ceb.2011.05.004
- Wang M, Kaufman RJ. Protein misfolding in the endoplasmic reticulum as a conduit to human disease. *Nature.* 2016;529(7586):326. doi:10.1038/nature17041
- Kadowaki H, Nishitoh H. Endoplasmic reticulum quality control by garbage disposal. *FEBS J.* 2019;286(2):232–240. doi:10.1111/febs.2019.286.issue-2
- Iurlaro R, Muñoz-Pinedo C. Cell death induced by endoplasmic reticulum stress. *FEBS J.* 2016;283(14):2640–2652. doi:10.1111/febs.13598
- Yang X, Shao H, Liu W, et al. Endoplasmic reticulum stress and oxidative stress are involved in ZnO nanoparticle-induced hepatotoxicity. *Toxicol Lett.* 2015;234(1):40–49. doi:10.1016/j.toxlet.2015.02.004
- Kuang H, Yang P, Yang L, Aguilar ZP, Xu H. Size dependent effect of ZnO nanoparticles on endoplasmic reticulum stress signaling pathway in murine liver. *J Hazard Mater.* 2016;317:119–126. doi:10.1016/j.jhazmat.2016.05.063
- Yin L, Dai Y, Cui Z, et al. The regulation of cellular apoptosis by the ROS-triggered PERK/EIF2alpha/chop pathway plays a vital role in bisphenol A-induced male reproductive toxicity. *Toxicol Appl Pharmacol.* 2017;314:98–108. doi:10.1016/j.taap.2016.11.013
- Kisin ER, Yanamala N, Farcas MT, et al. Abnormalities in the male reproductive system after exposure to diesel and biodiesel blend. *Environ Mol Mutagen.* 2015;56(2):265–276. doi:10.1002/em.v56.2
- Shang L, Nienhaus K, Nienhaus GU. Engineered nanoparticles interacting with cells: size matters. *J Nanobiotechnol.* 2014;12(1):5. doi:10.1186/1477-3155-12-5
- Hong F, Zhao X, Si W, et al. Decreased spermatogenesis led to alterations of testis-specific gene expression in male mice following nano-TiO<sub>2</sub> exposure. *J Hazard Mater.* 2015;300:718–728. doi:10.1016/j.jhazmat.2015.08.010

32. Lu X, Liu Y, Kong X, Lobie PE, Chen C, Zhu T. Nanotoxicity: a growing need for study in the endocrine system. *Small*. 2013;9(9–10):1654–1671. doi:10.1002/smll.201201517
33. Baek M, Chung H-E, Yu J, et al. Pharmacokinetics, tissue distribution, and excretion of zinc oxide nanoparticles. *Int J Nanomed*. 2012;7:3081.
34. Gao G, Ze Y, Zhao X, et al. Titanium dioxide nanoparticle-induced testicular damage, spermatogenesis suppression, and gene expression alterations in male mice. *J Hazard Mater*. 2013;258:133–143. doi:10.1016/j.jhazmat.2013.04.046
35. Toocheck C, Clister T, Shupe J, et al. Mouse spermatogenesis requires classical and nonclassical testosterone signaling. *Biol Reprod*. 2016;94(1):11. doi:10.1095/biolreprod.115.132068
36. Chen R, Huo L, Shi X, et al. Endoplasmic reticulum stress induced by zinc oxide nanoparticles is an earlier biomarker for nanotoxicological evaluation. *ACS Nano*. 2014;8(3):2562–2574. doi:10.1021/nm406184r
37. Schröder M, Kaufman RJ. The mammalian unfolded protein response. *Annu Rev Biochem*. 2005;74:739–789. doi:10.1146/annurev.biochem.73.011303.074134
38. Zhu G, Lee AS. Role of the unfolded protein response, GRP78 and GRP94 in organ homeostasis. *J Cell Physiol*. 2015;230(7):1413–1420. doi:10.1002/jcp.24923
39. Hetz C, Papa FR. The unfolded protein response and cell fate control. *Mol Cell*. 2018;69(2):169–181. doi:10.1016/j.molcel.2017.06.017
40. Zhang Q, Liu J, Chen S, et al. Caspase-12 is involved in stretch-induced apoptosis mediated endoplasmic reticulum stress. *Apoptosis*. 2016;21(4):432–442. doi:10.1007/s10495-016-1217-6
41. Urano F, Wang X, Bertolotti A, et al. Coupling of stress in the ER to activation of JNK protein kinases by transmembrane protein kinase IRE1. *Science*. 2000;287(5453):664–666. doi:10.1126/science.287.5453.664
42. Adams JM, Cory S. The BCL-2 arbiters of apoptosis and their growing role as cancer targets. *Cell Death Differ*. 2018;25(1):27. doi:10.1038/cdd.2017.161
43. Man SM, Kanneganti T-D. Converging roles of caspases in inflammasome activation, cell death and innate immunity. *Nat Rev Immunol*. 2016;16(1):7. doi:10.1038/nri.2015.7
44. Wang D. ZnO nanoparticle-induced oxidative stress triggers apoptosis by activating JNK signaling pathway in cultured primary astrocytes. *Nanoscale Res Lett*. 2014;9(1):12. doi:10.1186/1556-276X-9-589
45. Duan P, Hu C, Quan C, et al. 4-Nonylphenol induces apoptosis, autophagy and necrosis in sertoli cells: involvement of ROS-mediated AMPK/AKT-mTOR and JNK pathways. *Toxicology*. 2016;341-343:28–40. doi:10.1016/j.tox.2016.01.004
46. Eladak S, Moison D, Guerin MJ, et al. Effects of environmental Bisphenol A exposures on germ cell development and Leydig cell function in the human fetal testis. *PLoS One*. 2018;13(1):e0191934. doi:10.1371/journal.pone.0191934
47. Li L, Mu X, Ye L, Ze Y, Hong F. Suppression of testosterone production by nanoparticulate TiO<sub>2</sub> is associated with ERK1/2-PKA-PKC signaling pathways in rat primary cultured Leydig cells. *Int J Nanomedicine*. 2018;13:5909–5924. doi:10.2147/IJN.S175608
48. West LA, Horvat RD, Roess DA, Barisas BG, Juengel JL, Niswender GD. Steroidogenic acute regulatory protein and peripheral-type benzodiazepine receptor associate at the mitochondrial membrane. *Endocrinology*. 2001;142(1):502–505. doi:10.1210/endo.142.1.8052
49. Wang H, Wang Q, Zhao X-F, et al. Cypermethrin exposure during puberty disrupts testosterone synthesis via downregulating StAR in mouse testes. *Arch Toxicol*. 2010;84(1):53–61. doi:10.1007/s00204-009-0479-y
50. Hu M-C, Chiang EF-L, Tong S-K, et al. Regulation of steroidogenesis in transgenic mice and zebrafish. *Mol Cell Endocrinol*. 2001;171(1–2):9–14. doi:10.1016/S0303-7207(00)00385-3
51. Payne AH, Hales DB. Overview of steroidogenic enzymes in the pathway from cholesterol to active steroid hormones. *Endocr Rev*. 2004;25(6):947–970. doi:10.1210/er.2003-0030

## International Journal of Nanomedicine

### Publish your work in this journal

The International Journal of Nanomedicine is an international, peer-reviewed journal focusing on the application of nanotechnology in diagnostics, therapeutics, and drug delivery systems throughout the biomedical field. This journal is indexed on PubMed Central, MedLine, CAS, SciSearch®, Current Contents®/Clinical Medicine,

Journal Citation Reports/Science Edition, EMBase, Scopus and the Elsevier Bibliographic databases. The manuscript management system is completely online and includes a very quick and fair peer-review system, which is all easy to use. Visit <http://www.dovepress.com/testimonials.php> to read real quotes from published authors.

Submit your manuscript here: <https://www.dovepress.com/international-journal-of-nanomedicine-journal>

Dovepress